Journal of
Animal Health and Behavioural Science

El-Daly, J Anim Health Behav Sci 2017, 1:1

Research Article Open Access

The Histopathological, Ultrastructural and Immunohistochemical Effects of Intraperitoneal Injection with Titanium Dioxide Nanoparticles and Titanium Dioxide Bulk on the Liver of the Albino Mice

Amal A El-Daly*

Zoology Department, Faculty of Science, Benha University, Benha, Egypt

Abstract

Titanium Dioxide Nanoparticles (TiO_2-NPs) applications are widely used in the daily life and their potential toxicity to the living organism is necessary to be insured. The nanomaterial may or may not exhibit the same toxic potential as the original material. Therefore, this study used TiO_2-NPs and their original bulk to ensure their safety on the histology, immunohistochemistry and ultrastructure of the liver of male albino mice (*Mus musculus)*. For this purpose, 25 and 50 mg/kg b.wt.; 55 µm size; anatase TiO_2-NPs compared with 50 mg/kg b.wt.; 10^6 µm size; anatase TiO_2 micro-sized (bulk form) were daily injected intraperitoneally into the mice for ten successive days. The results showed numerous alterations in the liver of anatase TiO_2-NPs treated animals in a dose-dependent manner that were more than these shown in anatase TiO_2-bulk material. However, histopathological disruption of the normal cellular architecture of liver, vacuolization and congestion of blood capillary following higher doses of TiO_2-NPs exposure were revealed. In addition, quantitative analysis of both Bcl-2 and PCNA immunostaining density data showed significant increase as compared with the control indicating activation of apoptosis and proliferation in liver cells. Moreover, ultrastructural observation displayed dramatic potential alteration in nucleus, mitochondria, rER, numerous lysosomes, bile canaliculi and a Kupffer cell was detected. Besides, obvious agglomerations of TiO_2-NPs were taken up by hepatocytes cytoplasm and its organelles, nucleus and kupffer cells. These results show that TiO_2-NPs induced potential toxicity in mice liver following both doses used that varied severely when compared with TiO_2-bulk form. Therefore, it could be concluded that both tested doses of nano-anatase TiO_2 induced potential liver toxicity than the dose of bulk anatase TiO_2.

Keywords: Titanium dioxide nanoparticles (TiO_2-NPs); Histopathology; Immunohistochemistry; TEM; Mice; Liver

Introduction

Titanium Dioxide Nanoparticles (TiO_2-NPs) have been used in a wide variety of applications in the daily life. It may produce health risk when contact with humans and animals because it has unique physical and chemical properties. TiO_2-NPs has been beneficial in clinical medicine as a photosensitizer for photodynamic therapy and as a sunscreen [1,2], carrier platforms and clinical applications as well as drug delivery [3,4] and as a photothermal therapy for cancer [5,6]. Moreover, TiO_2 is used in many biomedical applications in the diagnosis and treatment of diseases [7,8].

Producing nanoparticles from the original material creates a new variety of molecular instruction by means of new different physicochemical properties. These nanoparticles properties come from their high surface-to-volume ratio as reported by Alarifi et al. [9]. The authors added that the higher percentage of atoms on their surface compared with bulk particles make them more reactive. Moreover, the small size and larger surface area of these particles are modified in comparison to the bulk of the same mass allows their dispersion into more cells, translocate into the organ and subcellular compartment create more toxic and inflammo-genic properties [10,11]. This toxicological alarm due to minute size smaller than cells and cellular organelles, allows them to penetrate these basic biological structures, disrupting their normal function [12]. However, Heinlaan et al. [13] showed that micro-TiO_2 was considered nontoxic because larger sized (bulk) TiO_2 that did not produce deleterious effects.

TiO_2-NPs were found to enter the blood stream in number of *in vivo* studies following exposure via inhalation, diet, intravenous or intraperitoneal injections [14-16] and it is associated with subsequent accumulation in the liver. Moreover, nano-TiO_2 can be transported into cells via phagocytosis then media-generating reactive oxygen species (ROS) that altered cellular redox balance towards oxidation producing abnormal function or cell death, lipid peroxidation, altered expression of genes, bind to the mitochondrial membrane so rising electron transport chain within the mitochondria, consequently, triggering the mitochondria-mediated apoptotic pathway [12,17-19]. In addition, titanium may exert its effect through some intracellular signalling pathways leading to expression of certain protein and biomolecules [20]. Therefore, histopathological changes, hepatocytes apoptosis, liver function damage and inflammatory cascade produced to the mouse liver with intraperitoneal injected high-doses with nanoparticulate anatase TiO_2 (5 µm) are closely related to significant alteration of the mRNA and protein expressions of several inflammatory cytokines [21,22].

Accordingly, TiO_2-NPs may interrupt the intracellular metabolic activity and the biological response of cells and a tissue producing potential toxicity that may vary from their bulk form. Therefore,

***Corresponding author:** Amal A El-Daly, Department of Zoology, Faculty of Science, Benha University, Benha, Egypt, Tel: +2 0127 544 8841; Fax: 002 013 322 2578; E-mail: ml_eldaly@yahoo.com

Received May 05, 2017; **Accepted** May 16, 2017; **Published** May 23, 2017

Citation: El-Daly AA (2017) The Histopathological, Ultrastructural and Immunohistochemical Effects of Intraperitoneal Injection with Titanium Dioxide Nanoparticles and Titanium Dioxide Bulk on the Liver of the Albino Mice. J Anim Health Behav Sci 1: 104.

the present study aimed to investigate the toxic potential of nano-TiO_2 particles compared with bulk TiO_2 particles in the liver of mice after 10 days of daily intraperitoneal administration. The hazards influence was evaluated at a level of light and electron microscopes by investigating histopathological changes, immunohistochemical reactivity and ultrastructure alterations of these nanoparticulate anatase TiO_2-treated mice.

Material and Methods

Characterization of TiO_2-NPs and bulk forms

In this study bulk Titanium dioxide (TiO_2 bulk) (Sigma Chemical Co. Aldrich Inc., UK) is used to compare its toxicity with the toxicity of Titanium Dioxides Nanoparticles (TiO_2-NPs). TiO_2-NP_s were prepared the Chemistry Department, Benha University, Egypt. Both particles have been characterized using three different techniques such as XRD, TEM and FT-IR in Figures 1-3, respectively. Crystal phase and size were evaluated using Bruker-D8 Advance Powder X-ray diffraction (XRD, Germany). Particle shape and morphology of TiO_2-NPs and TiO_2-bulk were assessed with JEM-2100 transmission electron microscope (TEM). Fourier transform infrared spectroscopy (IR) characterization of both particles were also carried out in the 400-4000 cm^{-1} frequency range and resolution 4 cm^{-1} using a Spectral Analyses Unit Thermo Fisher Nicolete IS10, USA. IR spectroscopy in the transmission mode gives qualitative information about the way in which the adsorbed molecules are bonded to the surfaces, as well as the structural information of solids.

Consequently, the average crystal size of TiO_2 nanoparticles was 55.3 µm anatase phase whereas the bulk TiO_2 assessed particle size 106.78 µm; anatase.

Animals and treatment

Male albino mice (*Mus musculus)* each weighing 25-30 g were used at commencement. They were kept in plastic cages under standard conditions with food and water provided *ad libitum*, and were maintained on a 12 h light/dark cycle. Humidity (55 ± 5%) and temperature (25 ± 2°C) was controlled. The animals were acclimatized for one week before the experimentation, then were randomly divided into four groups with five mice in each group: Group 1: Control group intraperitoneally (i.p.) injected daily with normal physiological saline

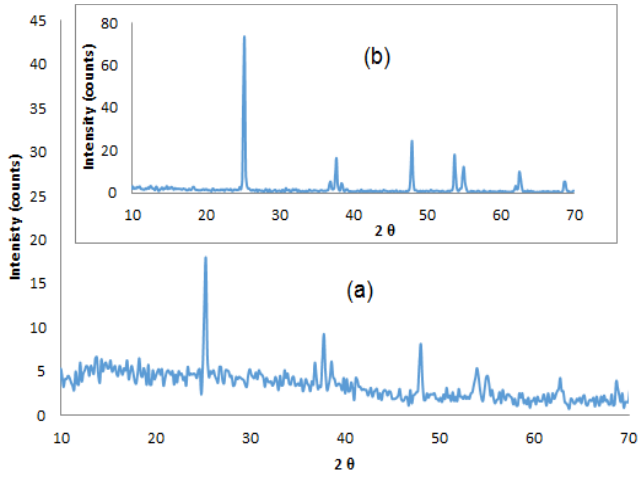

Figure 1: Shows X-ray diffraction (XRD) patters determined anatase phase structure of TiO_2 (a) nanoparticles; (b) bulk-particles.

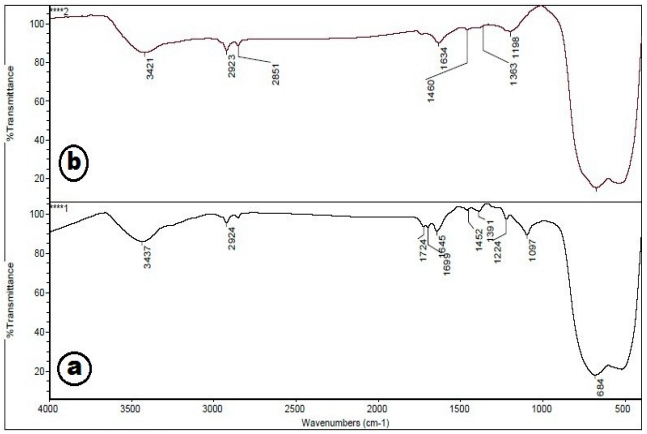

Figure 2: Shows IR spectra of TiO_2 (a) nanoparticles; (b) bulk-particles.

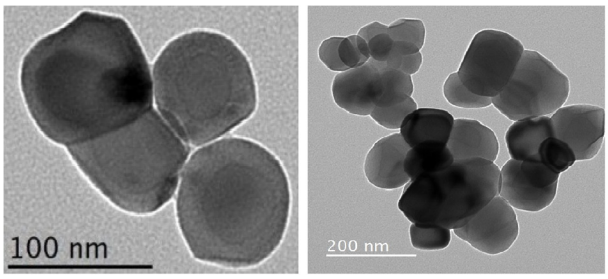

(a) Nanoparticles (b) Bulk particles

Figure 3: TEM images of both TiO_2 particles size and general morphology (a) nanoparticles; (b) bulk particles.

(0.9% $NaCl_2$). The following three groups (G2-G4) were i.p. injected with 25 and 50 mg/kg b. wt. of 55.3 µm; nano-anatase TiO_2 nanoparticles and 50 mg/kg b.wt. of 106.8 µm anatase TiO_2 bulk to compare the dose- and size related response to stress in biological activities in mice liver. Both types of particles were freshly prepared suspended in sterile physiological saline solution and given to the animals every day for 10 days. The animal protocols used in this study were in accordance with the Institutional Guidelines for the Care and Use of Animals approved by Menoufia University (MNSH156), Egypt.

Histopathological evaluation of liver

At the end of the experiment, the animals were anaesthetized using diethyl ether; their abdomens were opened, and the livers were then carefully removed and kept in 10% phosphate buffered formalin. After fixation, the tissues were dehydrated; cleared in xylene then embedded in paraffin wax. The tissue was cut (5-6 µm) and the sections were stained with the haematoxylin-eosin [23] and were studied by using Light Microscope (LM) for histopathological examination.

Immunohistochemical evaluation of Bcl-2 and PCNA expression

Bcl-2 and PCNA proteins were identified immunohistochemically by commercial monoclonal antibodies, namely anti-Bcl-2 (Dako, Cambridge, UK) and anti-PCNA (Dako, Cambridge, UK) in avidin-biotin complex using diaminobenzidine tetrahydrochloride (DAB) as a chromogen. 4 µ sections from each of the paraffin blocks of the liver samples onto salinized slides and processed eventually for primary and secondary antibodies incubation and then visualized using DAB

chromogen. Presence of a brown coloured end product at the site of the target antigen was indicative of positive reactivity. B cell lymphoma cell line was used as a positive control for Bcl-2 monoclonal antibody (Mab) and antibody was replaced by buffer in negative controls. Both positive and negative controls were run with each batch.

Imaging quantitative analysis of immunohistochemical staining: Quantitative analysis of immunostaining density of cytoplasmic Bcl-2 and nuclear PCNA antigen expression were determined when the slides were photographed using Olympus® digital camera with 0.5X photo adaptor, using 40X objectives and saved in TIFF. The result images were analyzed on Intel® Core I3® based computer using VideoTest Morphology® software (Russia) with a specific built-in routine for stain quantification and pixel intensity measurement. Additional confirmed analysis used was proliferation index of hepatocyte. It was expressed as the percentage counting numbers of PCNA positive stained nuclei in five consecutive microscopic random fields in the liver sections at 400X over the total number of the cells counted for the five fields [24].

Ultrastructure evaluation: Small pieces of the dissected livers were placed in the primary fixative of cold 2.5% glutaraldehyde in 0.1 mol/dm^3 cacodylate buffer and left overnight. The specimens were washed three times with 0.1 mol/dm cacodylate buffer (pH 7.2-7.4), then post-fixed for 1 h in 1% osmium tetraoxide, dehydrated through graded series of ethanol and embedded in Epon 812.The obtained ultrathin sections were stained with uranyl acetate and lead citrate [23], and examined and photographed with Jeol 1200 EX TEM, Tanta University, Egypt. A selected area in ultrathin sections examined using high-resolution TEM (JEM-2100 electron microscope, Mansoura University, Egypt) exposed to electrons diffraction practice to verify the presence of nano-crystallites in the hepatic tissue.

Statistical analysis: All the results were expressed as the means ± standard deviation. The data were analyzed using one way ANOVA followed by post-hoc tukey's test. $P<0.05$ was considered statistically significant. In the statistical comparison between the different groups, the significance of difference was tested using SPSS.

Results

Characterization of TiO_2 particles

The crystal size, shape and phase of both nano-particlesTiO_2 and bulk-particlesTiO_2 were determined by X-ray diffraction patterns. Figure 1a and 1b shows all prominent peaks for the crystal structure of anatase-TiO_2 also point out that the average sizes of both are 55.3 µm and 106.5 µm; respectively. TEM images of both TiO_2 particles size and general morphology shown in Figure 2a and 2b were in line with that obtained by XRD patterns as it reveals the same particles structure and size. Moreover, Figure 3a and 3b shows the FTIR spectrum of TiO_2 nano- and bulk-TiO_2 particles. IR spectroscopy in the transmission mode gives qualitative information about the way in which the adsorbed molecules are bonded to the surfaces as well as the structural information of solids material. The characteristic different peaks may be attributed to the presence of special groups in their structure.

Histopathological features of TiO_2 micro and nanoparticles

The histopathological changes in mouse liver following micro- and nano-TiO_2 particles treatment and control are shown in Figure 4. Section of control liver displayed normal structure with no abnormal changes (Figure 4a). 25 mg/kg b.wt. TiO_2-NPs exposure altered the regular hepatic architecture and hepatocyte apoptosis were detected. Highly vacuolated hepatocytes cytoplasm with obvious hyaline degeneration, nuclear pyknosis as well as fragmented nuclei was demonstrated (Figure 4b). Moreover, a haemorrhage appearance was observed in the narrow sinusoids due to aggregation of blood cells in parallel to congested blood capillaries. Kupffer cells appeared hypertrophied and their cytoplasm was darkly stained. On the other hand, higher dose of 50 mg/kg b.w TiO_2-NPs recorded more serious changes than in 25 mg/kg b.wt. TiO_2-NPs (Figure 4c). Plentiful pyknotic hepatic cells nuclei, irregularity in central veins and other was clearly destructed. Hyaline degeneration of the hepatocytes as well as obvious hyaline spots between the cells was detected. In contrast, animals treated with 50 mg/kg b.wt. bulk-TiO_2 for 10 days did not show these drastic hepatocytes variation compared with nano-particles treated groups (Figure 4d). This was more distinct in the subsequent ultrastructure appearance. However, 50 mg/kg b.wt. bulk-TiO_2 treated mice showed disruption of liver tissue strands as well as highly vacuolated cytoplasm, apoptic nuclei, shrinkage of hepatocytes and some of them appeared binucleated and slight congestion were observed. It was determined, administration of 50 mg/kg b.wt. TiO_2-bulk showed little alterations in liver tissue compared with the same dose of TiO_2 nanoparticles and even compared with lower dose (25 mg/kg b.wt. TiO_2).

Immunohistochemical analysis

Expression of Bcl-2 in liver tissue: Bcl-2 immunohistochemistry in Figure 5a-5d shows that the immunostained cells in mice liver i.p. treated with TiO_2-NPs and TiO_2 bulk for 10 days were intense compared with the control group. Data in Table 1 expressed as mean ± SD summarize the image analysis of anti-apoptotic Bcl-2 immunoreactivity intensity distribution in hepatocytes cytoplasm of the control and treated groups and the difference in this intensity between the treated groups themselves, 25 and 50 mg/kg b.wt. TiO_2-NPs-treated groups showed the intensity of anti-apoptotic Bcl-2 expression (165.5 ± 22.7 and 207.2 ± 29.0) respectively in the liver with statistically significant more higher increase compared with weak immunoreactivity in the control (73.5 ± 11.5) at $P<0.05$ or $P<0.001$. Moreover, this cytoplasmic intensity showed significant increase in liver of animals exposed to 50

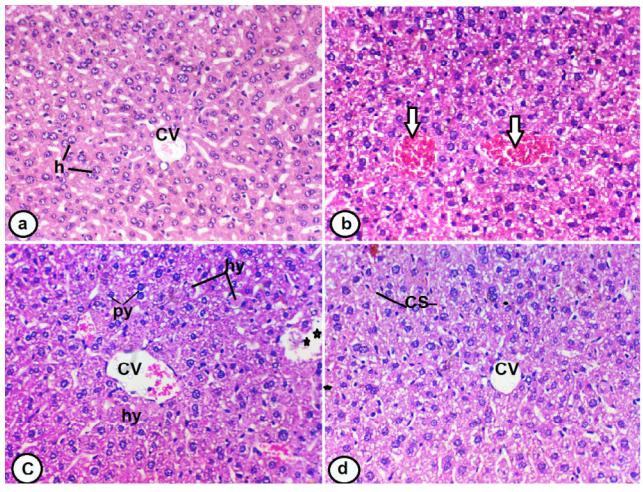

Figure 4: Photomicrographs of liver sections of mice from control and treated groups stained with haematoxylin and eosin displaying: (a) Control group with normal hepatocytes (h), nuclei (N) and normal central vein (CV). (b) 25 mg/kg b.wt. TiO_2-NPs treated mice displayed congested capillaries (arrows), vacuolated hepatocytes and pyknotic nuclei; (c) 50 mg/kg b.wt. TiO_2-NPs treated mice showed hyaline degeneration of hepatocytes, pyknotic nuclei (py), destructed central vein with aggregated cells (asterisk); (d) 50 mg/kg b.wt. bulk TiO_2 treated mice displaying cells degeneration and shrinkage (H&E, 400X).

		Control	25 mg/k b.wt. nano TiO_2	50 mg/kg b.wt. nano TiO_2	50 mg/kg b.wt. bulk TiO_2	P<0.001*
Mean ± SD	BCL-2	48.6 ± 4.9	140.3 ± 16.8**	194.2 ± 14.1**	83.4 ± 9.8*	
	PCNA	73.5 ± 11.5	165.5 ± 22.7**	207.2 ± 29.0**	118.0 ± 24.6*	

SD: Standard Deviation, P: Probability, significance value at <0.05.
Test used: One way ANOVA followed by post-hoc tukey.
*Significance (P<0.001) relative to the control.
**More highly significance (P<0.001) relative to the control.

Table 1: Quantitative distribution intensity of immunostain of both Bcl-2 and PCNA protein in liver after intraperitoneal administration with nano- and bulk TiO_2 expressed for successive 10 days as mean ± SD.

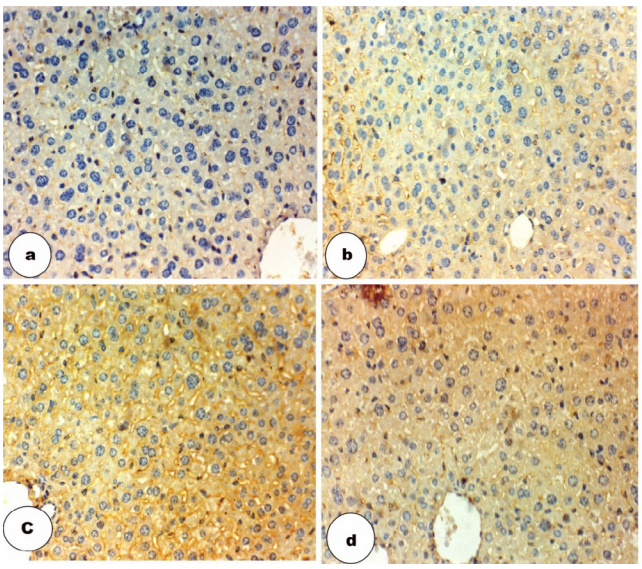

Figure 5: Photomicrographs of liver sections of mice from the control and the treated groups present immunohistochemical reaction of anti-apoptic Bcl-2 protein in hepatocytes cytoplasm: (a) Control with mild Bcl-2 reaction; (b) 25 mg/kg TiO_2-NPs; and (c) 50 mg/kg TiO_2-NPs treated mice display increased Bcl-2 reactivity in liver tissue, respectively in a significant dose-dependent manner. (d) Little increase Bcl-2 expression in bulk 50 mg/kg TiO_2 (Bcl-2, X400).

mg/kg b.wt., the cytoplasmic intensity of the TiO_2-bulk was 118.0 ± 24.6; this was significant (P<0.001) in relation to the control group. Bcl-2 immunoreaction showed also higher significant difference between the three treatments themselves (P<0.001).

Expression of PCNA in liver tissues: Image of PCNA immunohistochemistry in Figure 6a-6d, quantitative distribution of PCNA immunoreactivity data in Table 1 and percentage of positive cells count (proliferative index) in Histogram 1 showed similar results trends. Few PCNA positive cells were observed in the liver of the control mice (Figure 6a). Both nuclear PCNA immunostaining expression quantitative analyses in Table 1 and cells proliferation count in Histogram 1 in the liver of mice intraperitoneally injected with 25 and 50 mg/kg b.wt. TiO_2 nanoparticles revealed more high statistically significant increase compared with the control (P<0.05). This increase was dose-dependent. Meanwhile, sections stained with PCNA showed significant increase after 50 mg/kg b.wt. TiO_2 bulk particles treatment compared with the control group (P<0.05 or P<0.001). Thus, PCNA were more frequently present in the nano-TiO_2 treated groups rather than those of bulk TiO_2.

Ultrastructure alteration of hepatocytes: Liver of control mice showed normal hepatocytes enclosed spherical nuclei with normal nucleoli and well distributed chromatin consists of dense clumps of heterochromatin as well as lightly stained euochromatin (Figure 7a). The cytoplasm has numerous intact mitochondria, rough endoplasmic reticulum, Golgi apparatus and glycogen granules. However, the ultrastructure of hepatocyte from i.p. injected liver of 25 and 50 mg/kg TiO_2 nanoparticles and 50 mg/kg TiO_2 bulk particles treated groups displayed numerous alterations as compared to the control liver

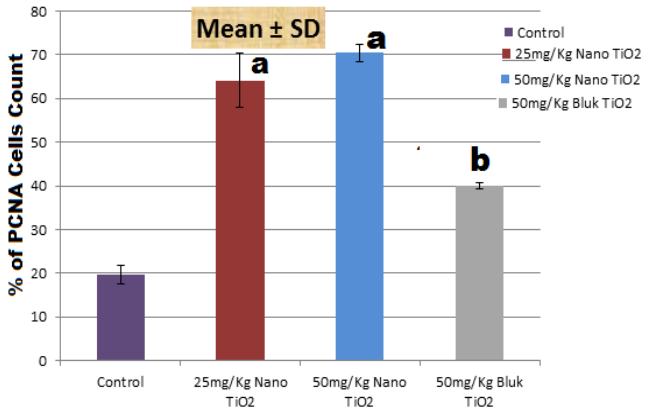

Histogram 1: The proliferative index as % of positive cells count. a: more highly significance, b: significance relative to the control (P<0.001).

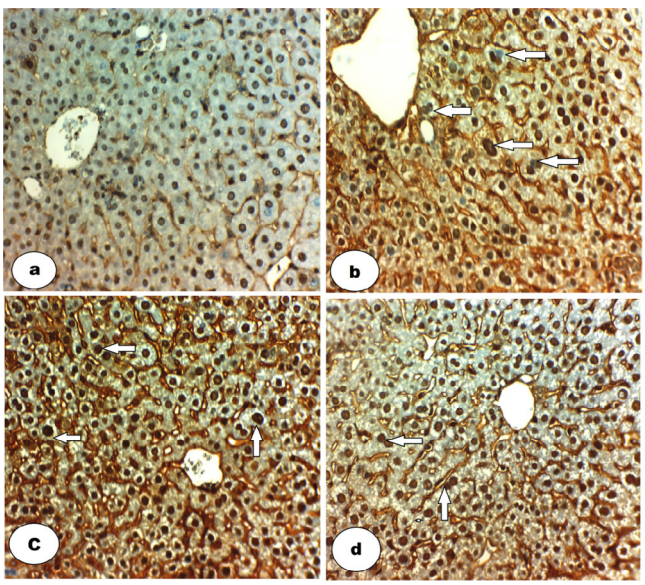

Figure 6: Photomicrographs of liver sections of mice from control and treated groups present immunohistochemical reaction of PCNA protein in hepatocytes nuclei: (a) Control group; (b) Mice treated with 25 mg/kg TiO_2-NPs; (c) 50 mg/kg TiO_2 NPs treated mice show increase in nuclear PCNA reactivity in liver tissue; (d) 50 mg/kg TiO_2 bulk treated mice show PCNA-positive nucleus (white arrow) (PCNA, X400).

(Figures 7 and 8). Similar with LM examination, exposure to 50 mg/kg TiO_2 bulk particle showed less deteriorations in the hepatocyte ultrastructure compared with the same dose of nanoparticles administration for the same period (10 days) and even compared with the lower dose.

On examination of the hepatocyte ultrastructure of the groups treated with both tested doses of TiO_2-NPs, accumulated titanium was observed. Therefore, when using high resolution TEM, the electron diffraction rings image formed inside the selected area of liver ultrathin section confirmed Titanium establishment in the hepatocyte (Figure 7b). The observed blurred rings in the dark-field view indicate the existence of TiO_2-NPs in distinct crystalline phase not amorphous accumulates within the cytoplasm mainly in lysosomes.

Moreover, the deterioration observed in hepatocyte of liver treated with higher dose of TiO_2-NPs (50 mg/kg) was more severe than that from the lower one (25 mg/kg) appeared in a dose-dependent manner. Moreover, the more interesting attending result was the enormous accumulation of TiO_2-NPs through the hepatocytes cytoplasmic matrix and organelles including mitochondrial matrix as electron-dense material and dilated rER, Kupffer cell, in perinuclear membrane therefore internuclear matrix after treatment with the two tested doses.

Consequently, liver treated with of 25 mg/kg b.wt. TiO_2-NPs showed damaged mitochoderia and rER and pale nucleus with irregular contour (Figure 7c). Another hepatocyte in Figure 7d show observable accumulated TiO_2-NPs in the cytoplasm, nucleus, nuclear envelope, deteriorated chromatin materials and vacuolated cytoplasm, destructed and dilated rough endoplasmic reticulum.

Exposure to higher dose of TiO_2-NPs (50 mg/kg b.wt.) showed swollen, decayed mitochondrial (M) without cristae and with obviously electron-dense material within its matrix may be nanoparticles collects. Destructed rER, cytoplasmic electron-dense deposited nanoparticles other than the perinuclear deposits and distinct two endosomes vacuoles were detected. Another image of 50 mg/kg b.wt. TiO_2-NPs exposure displayed dramatic nucleus with chromatin condensation and vacuolization, mitochondria, lipofuchsin depot and circular membraneous apoptic bodies. Bulk treated liver showed shrinkage hepatocytes with obvious cytoplasmic vacoulation and regular nuclear contour, destructed mitochondria and rER (Figure 8a-8d).

Among the deteriorations present in the cytoplasm after high dose of TiO_2-NPs exposure various inclusions related with hepatocytes damage visible in Figure 9a-9f. Firstly: Increase number of electron dense lysosomes with variable sizes signified TiO_2-NPs stored. Secondly; obvious membrane-enclosed circular structures apoptotic bodies more popular in both cytoplasm, nucleus and even in Kupffer cell indicated fragmentation and destructed organelles (Figures 8b and 9b). Thirdly: Electron-lucent lipid vacuoles in the hepatocyte cytoplasm following treatment with the lower dose and others electron-dense fat globules in the hepatocyte cytoplasm following treatment with the higher dose. Fourthly; circular large membranous inclusions of agglomerate vesicles like endosomes of nano-TiO_2-NPs may contribute to the clearance of particles from hepatocyte. Lastly: Presence of whorl-

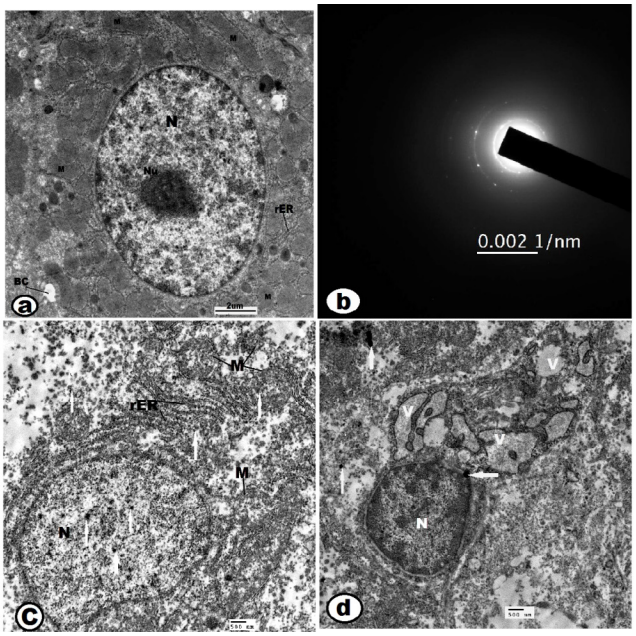

Figure 7: TEM micrographs of hepatocytes of the control mice and mice treated with TiO_2-NPs and bulk TiO_2; (a) A normal hepatocyte with normal nucleus (N), nucleoli (Nu), and mitochondria (M), rough endoplasmic reticulum (rER) (Scale bars=2 µm). (b) TEM micrograph shows the electron diffraction rings image formed as a result of nanocrystallites TiO_2 in the hepatocyte seen with high resolution. (c) 25 mg/kg TiO_2-NPs treated mice; portion of hepatocyte with more accumulation of nanoparticles material in lucent cytoplasm and nucleus (white arrow), thin nuclear envelope, destructed mitochondria and rER; and (d) another image of 25 mg/kg TiO_2-NPs treated mice markedly expanded rER, cytoplasmic vacuolization, accumulation of dense material in cytoplasm and adjacent to the nuclear envelope (white arrow) of the same treatment. (Scale bars=500 µm).

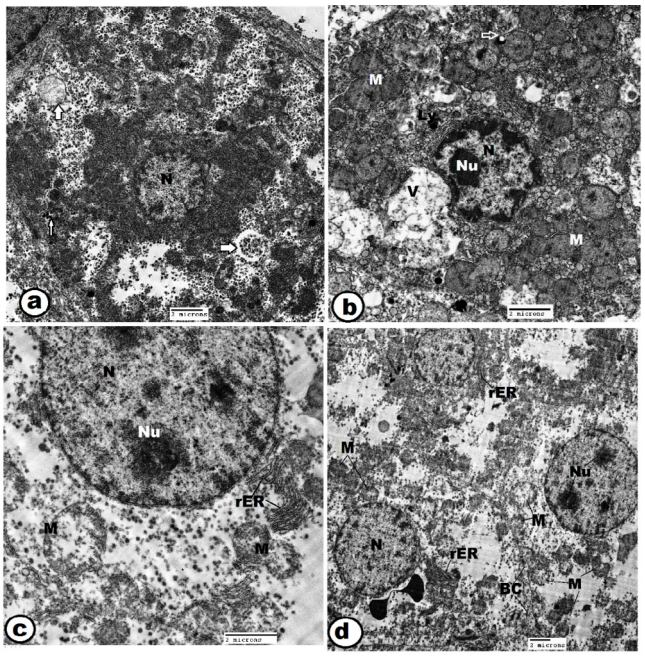

Figure 8: TEM micrographs of hepatocytes of mice treated with TiO_2-NPs and TiO_2 bulk particles. (a) 50 mg/kg TiO_2-NPs treated mice showing accumulation of TiO_2-NPs in the cytoplasmic and prinuclear, large membranous endosomes (arrows), damaged mitochondria (Scale bars=2 µm). (b) Another image of dramatic nucleus, precipitated TiO_2-NPs in damaged mitochondria and rER, apoptic bodies inclusions (Scale bars=2 µm). (c) 50 mg/kg TiO_2 bulk particles treated mice revealed three hepatocytes enclosed bile canaliculi with split microvilli, vacuolated cytoplasm (V), damaged mitochondria (M) and rER (Scale bars=2 µm). (d) Portion of the same treatment shows altered mitochondria and other organelles whereas little intact nucleus with prominent nucleoli and regular nuclear contour; parallel cisternae of rER (Scale bars=2 µm).

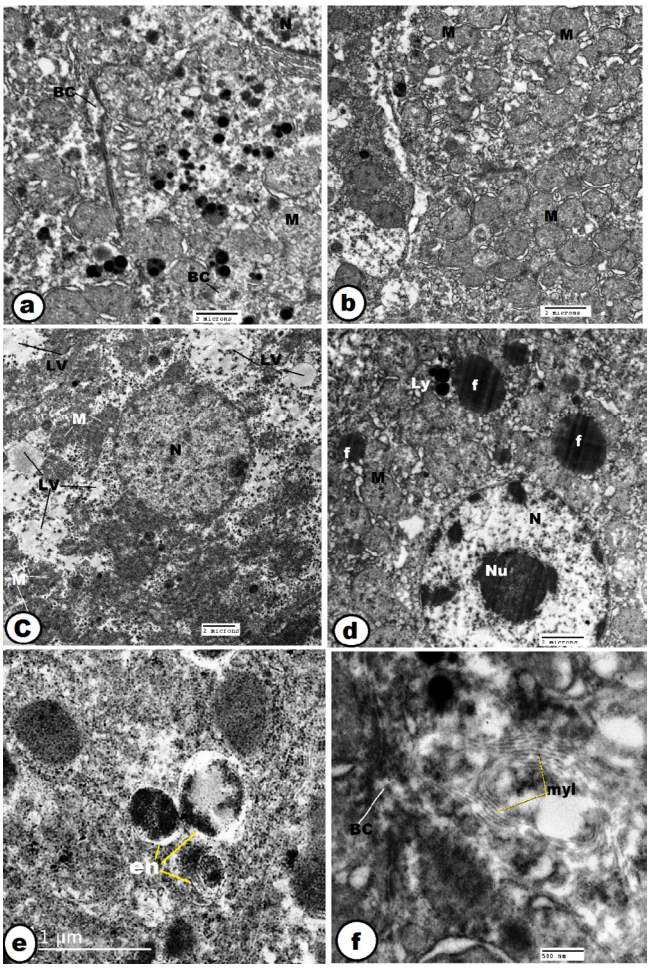

Figure 9: TEM micrographs of different inclusions in the hepatic cells from the TiO_2-NPs treated mice showing: (a) Abundant electron dense lysosomes with TiO_2-NPs accumulates (Scale bars=2 µm). (b) Numerous debris in a circular membranous inclusions as well as damaged mitochondria contained electron dense bodies inside it (Scale bars=2 µm). (c) Electron lucent lipid vacuoles in the hepatocyte cytoplasm (Scale bars=2 µm). (d) Electron dene fat globules (Scale bars=2 µm). (e) Large membranous endosomes filled with nanoparticles accumulations (Scale bars=1 µm). (f) Formation of myelin figure, damaged bile canaliculi and lysosome (Scale bars=500 µm).

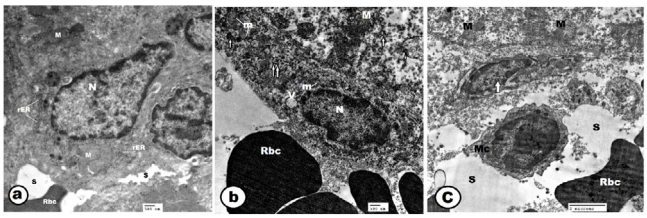

Figure 10: TEM micrographs of Kupffer cell from the control group and TiO_2-NPs treated group showing. (a) Normal Kupffer cell with normal organelles. (b) Kupffer cell from liver of mice treated with TiO_2-NPs showing hypertrophic cell laden with nanoparticles, plentiful inclusions and membranous vacuoles, split rER, endosomes, and a large number of lysosomes and endosome vesicles (arrow). (c) Dilated sinusoid with atrophied Kupffer and endothelial cells from bulk particles treated animals.

like membranous and multilamellar structures (myelin figure) in the hepatocyte cytoplasm of high dose treated liver (Figure 9a-9f).

As shown in Figure 10a-10c, appearance of hypertrophied Kupffer cells that was laden with titanium particles. Moreover, Kupffer cells showed plentiful inclusions and membranous vacuoles, split rough endoplasmic reticulum cisternae, endosomes, and a large number of lysosomes filled with TiO_2-NPs of different sizes that are observed inside endosome vesicles (arrow). These features did not found in that of the large particles tit (Figure 10c). Additionally, TEM image in Figure 11a-11d ultrastructure revealed abnormal bile canaliculi with obvious numerous inclusions with various sizes in the lumen indicated damaged microvilli after nano-anatase TiO_2 exposure (Figure 11b, 11c) compared to the control group (Figure 11a).These damage was not well identified in the bile canaliculi following bulk form treatment (Figure 11d).

Discussion

The present results show that the i.p. daily administration of 25 and 50 mg/kg b.wt. anatase TiO_2 nanoparticles for10 days induce liver toxicity in mice in a dose-response relation. So inversely, 50 g/kg b.wt. bulk TiO_2 particles treatment did not show these changes. These findings indicate that both particles enhanced impairment of liver functions. These alterations were detected at the level of histological, immunohistochemical and ultrastructure observations.

With respect to histopathological results, numerous hepatic alterations was detected following nano-anatase TiO_2 including irregular structure of hepatic tissue, apoptosis features as vacuolated cytoplasm and nuclear pyknosis, congested sinusoids and hyaline hepatocytes as well as hyaline spots were more evident after higher doses of TiO_2-NPs administration than in the lower dose compared with the control. However, alterations following exposure to both tested doses of TiO_2-NPs are more serious in the liver than in case of the bulk dose. This may be due to easily to enter into the hepatic tissue and cells and interact with proteins and biological systems leading to generation

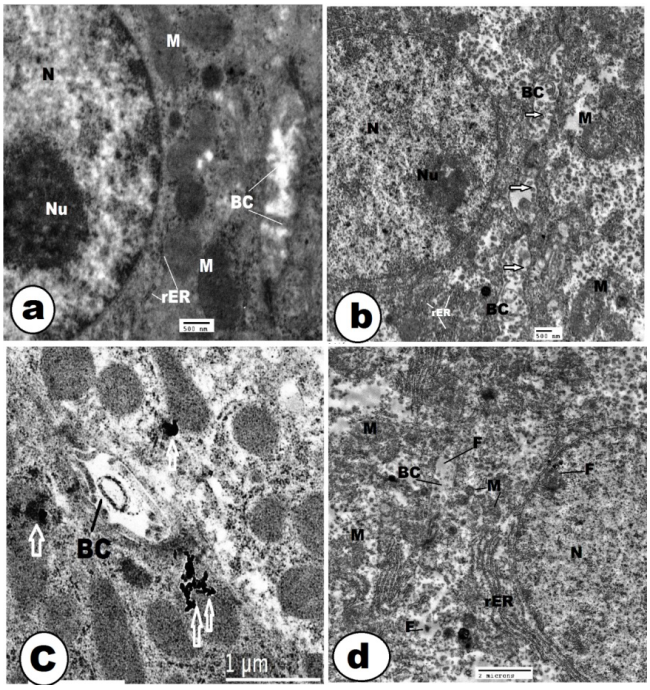

Figure 11: TEM micrographs showing bile canaliculi from control and treated mice: (a) Normal structure microvilli. (b and c) Bile canaliculi with obvious numerous abnormal inclusions with various sizes in the lumen indicated damaged microvilli after nano-anatase TiO_2 exposure. (d) These damage were not identified in the bile canaliculi following bulk form treatment (Figure 9d).

of Reactive Oxygen Species (ROS) generation which harmonized may submit these alterations in the hepatocytes. Moreover, accumulation of these particles in liver tissue through the experimental period must lead to this deterioration. Previous study added that the slow excretion of these particles from liver tissue will lead to the oxidative stress and initiated interaction with biological systems through different mechanisms of action that is not available for bulk materials [25-27]. Many authors showed that the small size of particles TiO_2-NPs give it more toxicity, and so they been more difficult to be remove [19,28,29]. Similarly, Shakeel et al. [29]; Chen et al. [14] showed that TiO_2 NPs recorded severe liver toxicity as necrosis, apoptosis and fibrosis in animals exposed to 100 and 150 mg TiO_2.

Moreover, exposure to TiO_2-bulk particles enhanced apoptosis with highly vacuolated cytoplasm with obvious hyaline degeneration, shrinkage, pyknosis and karyorrhexis, sinusoidal hemorrhages. Previous studies showed similar histological changes in the hepatic tissue of mice resulting from exposure to TiO_2NPs and TiO_2bulk. Ma et al. [21] reported that intraperitoneal injection of 100, 150 mg/kg b.wt. nano-anatase TiO_2-treated groups and 150 mg/kg b.wt. bulk TiO_2-treated group showed significant histopathological changes in the liver tissue, and 150 mg/kgb.w. bulk TiO_2- treated group induced histopathological changes and congestion of central veins in liver of mice. Wang et al. [30] observed that the hydropic degeneration around the central vein was prominent and the spotty necrosis of hepatocyte in the liver tissue of female mice post-exposure 2 weeks to the 5 g/kg b.wt. (80 nm) TiO_2 particles. Liu et al. [31] demonstrated that the titanium contents in livers of mice treated with intraperitoneal injections with 150 mg/kg b.wt. nano-anatase (5 nm) TiO_2 suspension was greater than the titanium contents in case of 150 mg/kg body weight of the bulk TiO_2. In the same line, Bermudez et al. [32] showed that inhaled TiO_2 nanoparticles can enhance pulmonary toxicity and translocation compared to the larger particles. Moreover, Alarifi et al. [9] added that the distinctive physicochemical properties of NPs are due to the high surface-to-volume ratio and extensive higher percentage of atoms on their surface compared with bulk particles makes them more reactive. This reactivity could lead to devastation of cellular component producing their toxic effects. Consequently, more Reactive Oxygen Species (ROS) generated following TiO_2-NPs treatment lead to an imbalance between oxidation and anti-oxidation and oxidative stress, and finally liver impairment [19,33]. On the other hand, Ma et al. [21] and Alarifi et al. [9] confirmed the TiO_2-NPs toxicity and the hepatic damage by the fluctuations in hepatic marker enzymes of serum aspartate transaminase (GOT) and ALP, hepatocyte apoptosis, swelling of blood vessels and mitochondrial damage and nuclear vacuolization.

In addition to the histological study, the Bcl-2 and PCNA immunohistochemistry reactivity were important to provide another aspect into TiO_2Ps toxicity mechanisms. The present results showed that intraperitoneal daily administration of both 25 and 50 mg/kg b.wt. TiO_2-NPs for 10 days caused more highly statistical significant increase ($p<0.05$ or 0.01) in Bcl-2 and PCNA immunoreactivity and distributional intensity as well as the proliferative index of PCNA stained cells compared to the control. These factors showed statistically significant increase in liver exposed to 50 mg/kg b.wt. of TiO_2 bulk particles compared to more highly significant increase observed after both doses of nanoparticles treatment. These increases may be due to over production of ROS resulting from interaction of these nanoparticles with DNA molecules leading to alteration in the expression of genes associated with cell proliferation and the cell cycle. Besides, resistance defence mechanisms to regeneration of hepatocytes damage and inhibit nano-TiO_2 induced toxicity. The increase of both Bcl-2 and PCNA overexpression confirm the histological alterations resulted in liver. Previous studies showed that PCNA is essential in replication and repair of DNA including nucleotide excision repair, the major pathway by which cells remove DNA damage introduced by a variety of chemical carcinogens [34,35]. In the same mannar, Tzung et al. [36] reported that Bcl-2 induced during proliferation of liver regeneration and may have a role in the control of normal cellular growth in addition to regulation of cell survival.

Therefore, molecular bases are an essential to liver pathogenesis following nano-TiO_2 administration. It increases the levels of cytokines, mRNA, and proteins related to inflammation including IL-1α, IL-1β, IL-6, IL-8, IFN-γ, and TNF-α by 5-20-fold [21,37]. The induction of proliferating cell nuclear antigen (PCNA) is required for both DNA replication and repair followed a similar spatial and temporal pattern to *p53* which reflect tumour-suppressor function of the *p53* gene [38]. Both have preventive effects of apoptosis on rat-colon tumorigenesis as reported by Zusman et al. [39] besides the hepatocytes proliferation is accompanied with patients at risk of cancer development in the liver [40]. Also, it was shown that increasing doses of nano-TiO_2 caused increase in liver DNA damage due to the binding of Ti^{4+} in the DNA nucleotide bases leading to changes in the expression levels of genes related to cell proliferation, signal transduction and the abnormal expression of important genes in the liver [22].

TEM findings in the current study revealed numerous important ultrastructure changes in liver cells following both the tested doses of anatase TiO_2-NPs (25 and 50 mg/kg b.wt TiO_2-NPs) did not found in bulk treated liver. Accumulation of nanoparticles was observed in the cytoplasmic matrix and organelles including mitochondrial matrix as electron-dense material and dilated rER in a dose-dependent manner. Dispersions of the particles in Kupffer cell were detected. Moreover, these accumulations were more obvious in perinuclear membrane and inter nuclear matrix. This accumulation may be due to the smaller particles sizes that are easier to enter the cells than larger size of the TiO_2 bulk form. Moreover, it may be due to the retaining long half-time of TiO_2 *in vivo* to be difficult to excrete and clearance, so the particle deposition in liver must lead to hepatic lesions [14]. However, the physical and chemical properties of nanomaterials are expected to cause significant effects on the behavior and properties of macromolecules, cells and body parts [41]. These findings are supported by a number of studies such as Zucker et al. [42] and Shukla et al. [43]. Moreover, TiO_2-NPs collection in largely membranous vesicles phagosome like structured or endosomes as well as numerous variable sizes of dense lysosomes in hepatocytes Figure 9 was detected. This result is in consistent with that previously obtained by Mano et al. [44]; Meena [45] and Schoelermann et al. [46]. They clarify that nano-TiO_2 can enter into cells by endocytosis and can be transferred between cells in direct contact with endosomes and lysosomes. Teubl et al. [47] revealed that TiO_2 nanoparticles were found in vesicles as well as freely distributed in the cytoplasm. Kettler et al. [48] added that the main mechanisms of nanoparticle uptake are based on macropinocytosis, receptor-mediated endocytosis, and phagocytosis. Similarly, another *in vitro* study by Gaiser et al. [49] using Ag NPs, noted that the particles were concentrated within membrane-bound vesicles point to either effective removal from the cytoplasm after diffusion through the membrane and incorporation into phagosomes or lysosomes, or uptake by mechanisms involving membrane incorporation of particles (e.g., endocytosis). Yanglong et al. [50] confirmed TiO_2 nanoparticle cytotoxicity by way of the conversion of TiO_2-NPs to ionic titanium in lysosomes.

The presence of TiO_2-NPs in these manners could facilitate generation and accumulation of ROS and oxidative stress that may be the main cause of the ultrastructure changes in the hepatocytes as swelling, perforations and disintegration of mitochondria, rER, irregularity in nuclear envelope and condensed as well as fragmented chromatin. The developed oxidative stress increases lipid peroxidation of membranes of mitochondria and rER permeability leading to disturbance in ATP and the intracellular calcium ions levels, then initiated several alterations. The mechanism by ROS due to nano-TiO_2 particles has been confirmed by another study by Long et al. [51] when showed that TiO_2 nanoparticles can bind to the mitochondrial membranes, causing collapse of the mitochondrial membrane electron transport chain and the generation of additional reactive O_2•- causes the structural damage to the mitochondria, permeable pore of its membrane to be open and apoptotic or necrotic pathways are activated. Meena [45] indicated that nano-TiO_2 particles are similar to hepatovirus, can enter liver cells or nuclei and bind to DNA cause changes in genetic information transfer and the inflammatory cascade. Also ROS produced after nano-TiO_2 may be due to interacting with these organelles decreased the levels of antioxidant enzymes. The damage in DNA and its strand might lead to changes in gene expression and even cell apoptosis [19]. The present findings also run parallel with those obtained by Jin et al. [52] and Xie et al. [53]. They found that TiO_2 nanoparticles because chromatin condenses fragments were directly leading to necrosis, the number of lysosomes to increase and some cytoplasmic organelles were damaged.

Among the ultrastructural observations in the present study is the presence of membrane apoptic bodies in the hepatocyte cytoplasm and nucleus and in Kupffer cell following 50 mg/kg TiO_2-NPs treatment suggesting destructed cellular components. Ma et al. [21] who found that 100 and 150 mg/kg b.w. nano-anatase TiO_2 caused apoptic body and vacuolization in hepatocyte of the mouse liver. Shi et al. [54] and Shukla et al. [43] explained that the increase the quantity of apoptotic bodies by nano-TiO_2 resulting from lipid peroxidation and oxidative stress, increased expression levels of *p53*, changes in the ratio of Bax/Bcl-2, which leads to the release of apoptotic protease activating factor (Apaf-1) that bind to cytochrome C leading to the formation of apoptotic bodies. This confirms that the present histological, immunohistochemical and ultrastructure observations run in parallel line to explain the mechanism of action after nano-TiO_2 toxicity.

Among the important abnormal features following intraperitoneal administration of different doses TiO_2-NPs is the presence of variable sized fat globules. This finding is in agreement with the results obtained by Alarifi et al. [9] and Sarhan and Hussein [55]. But the present finding differs from them in which these fat globules were lucent in 25 mg/kg TiO_2-NPs treatment but it was dense in case of 50 mg/kg TiO_2-NPs. These variations suggesting that change in doses of TiO_2-NPs had unlike ability to inhibits fatty acid oxidation induced by ROS and oxidative stress associated with lipid metabolism as well as changes in the expression of genes involved in the biosynthetic pathways of both cholesterol and lipid metabolism as reported by Cui et al. [22]. In the same manner, a multilamellar cytoplasmic structure (myelin figures) detected in this study when mice were exposed to 50 mg/kg TiO_2-NPs might be due to lipid peroxidation of the cell organelles membranes indicating markers of cell death. Therefore, there are relations between the presences of this multilamellar structure with various pathological conditions such as toxic drug effects as reported by Schulze-Osthoff et al., [56]; Hariri et al., [57] as well as lipid-loaded cells deriving either from free or esterified cholesterol cells as reported by Bobryshev [58] and caspase activity and polar lipid accumulation that are linked with the cytotoxicity of oxysterols [59].

Destruction of the bile canaliculi microvilli following TiO_2-NPs that was detected in the present results may be due to oxidative stress on the liver cells as it is the main organ that excreted the toxic substances through the bile canaliculi. Shakeel et al. [29] reported that bile is a fluid secreted from liver cells and helps body to split fat, process cholesterol and get rid of toxins, so if the bile duct is injured, alkaline phosphatase can be get backed up and leak out from the liver.

Therefore, destruction in the bile canaliculi microvilli, fat globules, myelin figure formation, and membrane peroxidation of the cellular constituents, ROS and the disturbance of intracellular calcium concentration are related factors confirm each other with TiO_2-NPs toxicity. Secondly, the inductions of oxidative stress together with unique physical and chemical properties, including magnetic, catalytic, electrical, and mechanical features of nano-TiO_2 exhibit compared with the bulk materials [60]. Another suggestion by Fröhlich and Roblegg [61] showed that the nanoparticles taken up, due to their charged reactive surface, facilitating the uptake of other unwanted molecules. Finally; Cho et al. [62] added that combined with these toxicity data, kinetics data can provide the actual concentration of nanoparticles as they interact with biological systems.

From these results, it could conclude that TiO_2-NPs stimulate hepatotoxicity in male albino mice in a dose-dependent manner at the level of histological, immunohistochemical and ultrastructure examinations. Moreover, higher dose of TiO_2-NPs displayed important alterations in liver tissue as compared to the same dose of bulk particles for the same period indicate toxic effects of nanoTiO_2 on liver. Further studies must be necessary using other techniques to study nano-TiO_2 effects on liver activity.

Acknowledgment

The author is very gratitude to Dr. Islam M.I. Moustafa at Faculty of Science, Benha University for preparing the material used for this study in his Laboratory.

Conflict of Interest

The author declares that she has no conflict of interest.

References

1. Wang JX, Liu Y, Jiao F, Lao F, Li W, et al. (2008) Time-dependent translocation and potential impairment on central nervous system by intranasally instilled TiO_2 nanoparticles. Nanotoxicology 254: 82-90.
2. Zeng L, Pan Y, Tian Y, Wang X, Ren W, et al. (2015) Doxorubicin-loaded NaYF4:Yb/Tm-TiO_2 inorganic photosensitizers for NIR-triggered photodynamic therapy and enhanced chemotherapy in drug-resistant breast cancers. Biomaterials 57: 93-106.
3. Lehner R, Wang X, Marsch S, Hunziker P (2013) Intelligent nanomaterials for medicine: carrier platforms and targeting strategies in the context of clinical application Nanomed. Nanotechnology 9: 742-757.
4. Du Y, Ren WZ, Li YQ, Zhang Q, Zeng LY, et al. (2015) The enhanced chemotherapeutic effects of doxorubicin loaded PEG coated TiO_2 nanocarriers in an orthotopic breast tumor bearing mouse model. J Mater Chem B 3: 1518-1528.
5. Yamaguchi S, Kobayashi H, Narita T, Kanehira K, Sonezaki S, et al. (2010) Novel photodynamic therapy using water-dispersed TiO_2-polyethylene glycol compound: evaluation of antitumor effect on glioma cells and spheroids *in vitro*. Photochem Photobiol 86: 964-971.
6. Ren W, Yan Y, Zeng L, Shi Z, Gong A, et al. (2015) A near infrared light triggered hydrogenated black TiO_2 for cancer photothermal therapy. Adv Healthc Mater 4: 1526-1536.
7. Duncan R (2006) Polymer conjugates as anticancer nanomedicines. Nat Rev Cancer 6: 688-701.
8. Rytting E, Nguyen J, Wang X, Kissel T (2008) Biodegradable polymeric nanocarriers for pulmonary drug delivery. Expert Opin Drug Deliv 5: 629-639.

9. Alarifi S, Ali D, Al-Doaiss AA, Ali BA, Ahmed M, et al. (2013) Histologic and apoptotic changes induced by titanium dioxide nanoparticles in the livers of rats. Int J Nanomed 8: 3937-3943.

10. Duffin R, Tran L, Brown D, Stone V, Donaldson K (2007) Proinflammogenic effects of low-toxicity and metal nanoparticles *in vivo* and *in vitro*: highlighting the role of particle surface area and surface reactivity. Inhal Toxicol 19: 849-856.

11. Geiser M, Kreyling WG (2010) Deposition and biokinetics of inhaled. Part Fibre Toxicol 7: 2.

12. Buzea C, Blandino IIP, Robbie K (2007) Nanomaterials and nanoparticles: Sources and toxicity. Biointerphases 2: 17.

13. Heinlaan M, Ivask A, Blinova I, Dubourguier HC, Kahru A (2008) Toxicity of nanosized and bulk ZnO, CuO and TiO_2 to bacteriaVibrio fischeri and crustaceans *Daphnia magna* and *Thamnocephalus platyurus*. Chemosphere 71: 1308-1316.

14. Chen J, Dong X, Zhao J, Tang G (2009) *In vivo* acute toxicity of titanium dioxide nanoparticles to mice after intraperitioneal injection. J Appl Toxicol 29: 330-337.

15. Geiser E, Sandmann P, Jancke L, Meyer M (2010) Refinement of metre perception-training increases hierarchical metre processing. Eur J Neurosci 32: 1979-1985.

16. Schleh C, Semmler-Behnke M, Lipka J, Wenk A, Hirn S, et al. (2012) Size and surface charge of gold nanoparticles determine absorption across intestinal barriers and accumulation in secondary target organs after oral administration. Nanotoxicology 6: 36-46.

17. Cui Y, Gong X, Duan Y, Li N, Hu R, et al. (2010) Hepatocyte apoptosis and its molecular mechanisms in mice caused by titanium dioxide nanoparticles. J Hazardous Mat 183: 874-880.

18. Li N, Ma L, Wang J, Zheng L, Liu J, et al. (2010) Interaction Between Nano-Anatase TiO_2 and Liver DNA from Mice *In vivo*. Nanoscale Res Lett 5: 108-115.

19. Hong J, Zhang YQ (2016) Murine liver damage caused by exposure to nano-titanium dioxide. Nanotechnology 27: 112001.

20. Nakashima Y, Sun DH, Trindade MC, Maloney WJ, Goodman SB, et al. (1999) Signaling pathways for tumor necrosis factor-alpha and interleukin-6 expression in human macrophages exposed to titanium-alloy particulate debris *in vitro*. J Bone Joint Surg Am 81: 603-615.

21. Ma L, Zhao J, Wang J, Liu J, Duan Y, et al. (2009) The acute liver injury in mice caused by nano-anatase TiO_2. Nanoscale Res Lett. 4: 1275-1285.

22. Cui Y, Liu H, Ze Y, Zengli Z, Hu Y, et al. (2012) Gene expression in liver injury caused by long-term exposure to titanium dioxide nanoparticles in mice. Toxicol Sci 128: 171-185.

23. Bancroft JD, Stevens A (1999) Theory and Practice of Histological Techniques (4^{th} edn.). Churchill-Livingstone, London.

24. Ojanguren I, Ariza A, Llatjós M, Castell`a E, Mate JL, et al. (1993) Proliferating cell nuclear antigen expression in normal, regenerative and neoplastic liver: A fine needle aspiration cytology and biopsy study. Hum Pathol 24: 905-908.

25. Oberdörster G, Oberdörster E, Oberdörster J (2005) Nanotoxicology: an emerging discipline evolving from studies of ultrafine particles. Environ Helth Perspect 113: 823-839.

26. Xiong D, Fang T, Yu L, Sima Z, Zhu W (2011) Effects of nano-scale TiO_2, ZnO and their bulk counterparts on zebrafish: Acute toxicity, oxidative stress and oxidative damage. Sci Total Environ 409: 1444-1452.

27. Vasantharaja D, Ramalingam, V, Reddy GA (2015) Oral toxic exposure of titanium dioxide nanoparticles on serum biochemical changes in adult male wistar rats. Nanomedicine J 2: 46-53.

28. Hua J, Vijver MG, Ahmad F, Richardson MK, Peijnenburg WJGM (2014) Toxicity of different-sized copper nano- and submicron particles and their shed copper ions to zebrafish embryos. Environ Toxicol Chem 33: 1774-1782.

29. Shakeel M, Jabeen F, Qureshi NA, Fakhr-e-Alam M (2016) Toxic Effects of Titanium Dioxide Nanoparticles and Titanium Dioxide Bulk Salt in the Liver and Blood of Male Sprague-Dawley Rats Assessed by Different Assays. Biol Trace Elem Res 173: 405-426.

30. Wang J, Zhou G, Chen C, Yu H, Wang T, et al. (2007) Acute toxicity and biodistribution of different sized titanium dioxide particles in mice after oral administration. Toxicol Lett 168: 176-185.

31. Liu H, Ma L, Zhao J, Liu J, Yan J, et al. (2009) Biochemical toxicity of nanoanatase TiO_2 particles in mice. Biol Trace Elem Res 129: 170-180.

32. Bermudez E, Mangum JB, Wong BA, Asgharian B, Hext PM, et al. (2004) Pulmonary responses of mice, rats, and hamsters to subchronic inhalation of ultrafine titaniumdioxide particles. Toxicol Sci 77: 347-357.

33. Johnston HJ, Hutchison GR, Christensen FM, Peters S, Hanki S, et al. (2009) Identification of the mechanisms that drive the toxicity of TiO_2 particulates: the contribution of physicochemical characteristics. Part Fibre Toxicol 6: 33.

34. Essers, J, Theil A, Baldeyron C, van Cappellen WA, Houtsmuller AB, et al. (2005) Nuclear Dynamics of PCNA in DNA Replication and Repair. Mol Cellul Biol 25: 9350-9359.

35. Hoogervorst EM, van Steeg H, de Vries A (2005) Nucleotide excision repair- and p53-deficient mouse models in cancer research. Mutat Res 574: 3-21
.

36. Tzung SP, Fausto N, Hockenbery DM (1997) Expression of *Bcl-2* Family during Liver Regeneration and Identification of Bcl-x as a Delayed Early Response Gene. Am J Pathol 150: 1985-1995.

37. Cui Y, Liu H, Zhou M, Duan Y, Li N, et al. (2011) Signaling pathway of inflammatory responses in the mouse liver caused by TiO_2 nanoparticles. J Biomed Materials Res Part A 96: 221-229.

38. Hall PA, McKee PH, Menage HDP, Dover R, Lane DP (1993) High levels of p53 protein in UV-irradiated normal human skin. Oncogene 8: 203-207.

39. Zusman I, Reifen R , Livni O, Smirnoff P, Gurevich P, et al. (1997) Role of apoptosis, proliferating cell nuclear antigen and p53 protein in chemically induced colon cancer in rats fed corncob fiber treated with the fungus Pleurotus ostreatus. Anticancer Res 17: 2105-2113.

40. Azzaroli F, Colecchi A, Iodato F, Trere D, Reggiani MLB, et al. (2006) A statistical model predicting high hepatocyte proliferation index and the risk of developing hepatocellular carcinoma in patients with hepatitis C virus-related cirrhosis. Aliment Pharmacol Ther 24: 129-136.

41. Saman S, Moradhaseli S, Shokouhian A, Ghorbani M (2013) Histopathological effects of ZnO nanoparticles on liver and heart tissues in Wistar rats. Adv Biores 4: 83-88.

42. Zucker RM, Massaro EJ, Sanders KM, Degn LL, Boyes WK (2012) Detection of TiO_2 nanoparticles in cells by flow cytometry Methods. Mol Biol 906: 497-509.

43. Shukla RK, Kumar A, Gurbani D, Pandey AK, Singh S, et al. (2013) TiO_2 nanoparticles induce oxidative DNA damage and apoptosis in human liver cells. Nanotoxicology 7: 48-60.

44. Mano SS, Kanehira K, Sonezaki S, Taniguchi A (2012) Effect of polyethylene glycol modification of TiO_2 nanoparticles on cytotoxicity and gene expressions in human cell lines. Int J Mol Sci 13: 3703-3717.

45. Meena R (2012) Oxidative stress mediated cytotoxicity of TiO_2 nano anatase in liver and kidney of Wistar rat. Toxico Environ Chem 94: 146-163.

46. Schoelermann J, Burtey A, Allouni ZE, Gerdes HH, Cimpan MR (2015) Contact-dependent transfer of TiO_2 nanoparticles between mammalian cells. Nanotoxicology 10: 204-215.

47. Teubl BJ, Leitinger G, Schneider M, Lehr CM, Fröhlich F, et al. (2015) The buccal mucosa as a route for TiO_2 nanoparticle uptake. Nanotoxicology 9: 253-261.

48. Kettler K, Veltman K, van de Meent D, Hendriks AJ (2014) Cellular uptake of nanoparticles as determined by nanoparticle properties, experimental conditions and cell type. Environ Toxicol Chem 33: 481-492.

49. Gaiser BK, Hirn S, Kermanizadeh A, Kanase N, Fytianos K, et al. (2013) Effects of Silver Nanoparticles on the Liver and Hepatocytes *In vitro*. Toxicol Sci 131: 537-547.

50. Yanglong Z, John WE, Li C (2012) Titanium dioxide (TiO_2) nanoparticles preferentially induce cell death in Transformed cells in Bak/Bax-independent fashion. PLoS One 7: e50607.

51. Long TC, Saleh N, Tilton RD, Lowry GV, Veronesi B (2006) Titanium dioxide (P25) produces reactive oxygen species in immortalized brain microglia (BV2): implications for nanoparticle neurotoxicity. Environ Sci Technol 40: 4346-4352.

52. Jin CY, Zhu BS, Wang XF, Lu QH (2008) Cytotoxicity of titanium dioxide nanoparticles in mouse fibroblast cells. Chem Res Toxicol 21: 1871-1877.

53. Xie GP, Wang C, Sun J, Zhong GR (2011) Tissue distribution and excretion of intravenously administered titanium dioxide nanoparticles. Toxicol Lett 205: 55-61.

54. Shi H, Magaye R, Castranova V, Zhao J (2013) Titanium dioxide nanoparticles: a review of current toxicological data. Part Fibre Toxicol 10: 15.

55. Sarhan OMM, Hussein RM (2014) Effects of intraperitoneally injected silver nanoparticles on histological structures and blood parameters in the albino rat. Internat J Nanomed 9: 1505-1517.

56. Schulze-Ostho VK, Bakker AC, Vanhaesebroeck B, Beyaert R, Jacob WA, et al. (1992) Cytotoxic activity of tumor necrosis factor is mediated by early damage of mitochondrial functions. J Biol Chem 267: 5317-5323.

57. Hariri M, Millane G, Guimond MP, Guay G, Dennis JW, et al. (2000) Biogenesis of multilamellar bodies via autophagy. Mol Biol Cell 11: 255-268.

58. Bobryshev YV (2006) Monocyte recruitment and foam cell formation in atherosclerosis. Micron 37: 208-222.

59. Vejux A, Kahn E, Ménétrier F, Montange T, Lherminier J, et al. (2007) Cytotoxic oxysterols induce caspase-independent myelin figure formation and caspase-dependent polar lipid accumulation. Histochem Cell Biol 127: 609-624.

60. Wang J, Wang L, Fan Y (2016) Adverse biological effect of TiO_2 and hydroxyapatite nanoparticles used in bone repair and replacement. Int J Mol Sci 17: 798.

61. Fröhlich E, Roblegg E (2012) Models for oral uptake of nanoparticles in consumer products. Toxicology 291: 10-17.

62. Cho WS, Kang BC, Lee JK, Jeong J, Che JH, et al. (2013) Comparative absorption, distribution, and excretion of titanium dioxide and zinc oxide nanoparticles after repeated oral administration. Part Fibre Toxicol 10: 9.